Observation of the First-Order Raman Scattering in $SrTiO_3$ Thin Films

A. A. Sirenko, I. A. Akimov,* J. R. Fox, A. M. Clark, Hong-Cheng Li,† Weidong Si, and X. X. Xi
Department of Physics, The Pennsylvania State University, University Park, Pennsylvania 16802
(Received 22 September 1998)

We have studied lattice dynamic properties of $SrTiO_3$ thin films from 5 to 300 K using metal-oxide bilayer Raman scattering. First-order zone-center optical phonons, symmetry forbidden in single crystals, have been observed in the thin films, indicating strain-induced lowering of symmetry. The asymmetric line shape of the TO_2 phonon is interpreted as evidence for micropolar regions in the thin films, likely due to oxygen vacancies. The optical phonon lines and the asymmetry persist up to room temperature. [S0031-9007(99)09277-7]

PACS numbers: 77.84.Dy, 63.20.Ls

Lattice dynamics is of central significance in the studies of the quantum paraelectric $SrTiO_3$ (STO). Müller *et al.* [1] proposed that the low temperature state of STO is a coherent quantum state associated with a rotonic minimum in the TA mode. Various anomalies exhibited by STO at ~35 K were suggested as a possible indication of a transition to this state [2]. In STO thin films, we have reported quantum fluctuation and phase transition behaviors that are different from those in the single crystals [3]. Stress has been suggested as the primary cause, although the relative roles of lattice mismatch and oxygen vacancies remains an open question. For applications in frequency and phase agile electronics [4], reducing the dielectric loss of STO thin films is crucial. For single-crystal STO, the loss is primarily related to the phonon absorption involving the soft modes [5]. However, due to difficulties in Raman measurements in transparent thin films, little has been studied of the soft and hard modes in STO thin films. Recently we have used the metal-oxide bilayer Raman scattering (MOBRS) technique, in which conducting metal oxides are utilized as light reflectors, and were able to observe Raman signals from the STO thin films at room temperature [6]. In this paper, we report on MOBRS studies of STO thin films from 5 to 300 K. Strong peaks corresponding to the zone-center optical phonons symmetry forbidden in the bulk were clearly observed. The TO_2 phonon shows a strong Fano asymmetry, which we attribute to the interaction of the polar mode with polarization fluctuations in micropolar regions.

STO films were grown by pulsed laser deposition (see Ref. [4] for details). Between the single-crystal $LaAlO_3$ (LAO) substrate and the STO layer, a 0.35 μm metallic $SrRuO_3$ (SRO) film was grown to screen Raman signals from the LAO substrates. The lattice constant mismatch between the STO and SRO layers is very small (0.64%), resulting in a slightly tensile in-plane stress in the STO films. X-ray diffraction measurement indicates that the STO films have a tetragonal structure with the c axis lying in the film plane [7]. Narrow full width at half maximum (FWHM) is found in both the Bragg peaks (~0.1°) and the rocking curves (~0.16°). Low-frequency (50 Hz–1 MHz) dielectric measurements show low dielectric losses [4] and qualitatively different quantum fluctuation behaviors from that of single crystals [3].

For Raman measurement, the sample was attached to the cold finger inside an optical He-flow cryostat. The 5145 Å line (2.4 eV) of an Ar^+-ion laser was used for excitation, and the pumping power was below 0.5 W/cm^2. Raman spectra were measured with a SPEX Triplemate spectrometer equipped with a charge-coupled device detector cooled with liquid nitrogen. The resolution was about 1.5 cm^{-1}. Linear polarization of the Raman signal was analyzed in the conventional backscattering configuration (laser beam and scattered light perpendicular to the sample plane). The Porto's notation is used to denote the scattering configurations. The z axis is perpendicular to the film plane, and the x, x', y, and y' axes are parallel to the [100], [110], [010], and $[1\bar{1}0]$ axes of the LAO structure, respectively.

Bulk STO crystals have a centrosymmetric structure: cubic at high temperatures and tetragonal below T_a = 105 K. The zone-center optical phonons are of odd parity, and consequently are not Raman active [8]. The results of the STO thin films are very different. In Fig. 1, Raman spectra of three STO films of different thicknesses measured at $T = 5$ K are shown together with that of a single crystal. By comparing with the hyper-Raman results of bulk single crystals [9,10], where optical phonons are active, we identify the strong peak at 170 cm^{-1} as due to the TO_2, the weak peak at 264 cm^{-1} to the silent TO_3, and the strong peak at 545 cm^{-1} to the TO_4 phonons. These peaks can be observed up to room temperature. The FWHM of the $TO_{2,4}$ phonons increases with temperature, changing in the range of 10–20 cm^{-1}, about 4 times broader than that in bulk STO. Relatively weak features in the Raman spectrum marked with stars at 118, 221, 247, 386, and 408 cm^{-1} are related to the SRO buffer layer [11]. In contrast, the Raman spectrum of the STO single crystal is characterized by the second-order scattering signal and the structural modes denoted by the letter R. The structural modes become Raman

 0031-9007/99/82(22)/4500(4)$15.00

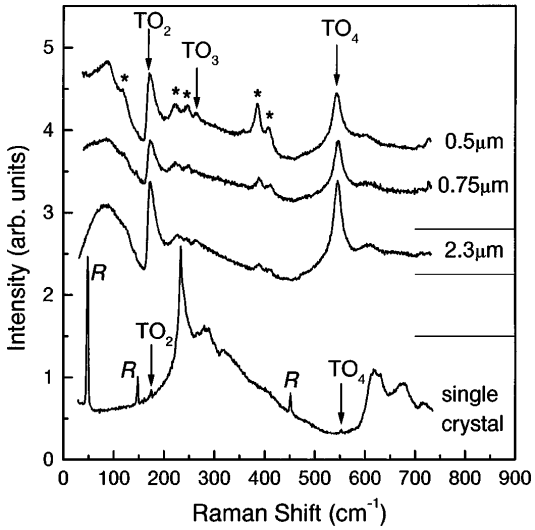

FIG. 1. Normalized Raman spectra of STO films and a single crystal measured at $T = 5$ K with excitation at 2.4 eV. The spectra are taken in $z(x', x')\bar{z}$ configuration. The STO film thickness is given next to each spectrum. The spectra were vertically shifted for clarity. The horizontal solid lines indicate the respective zero-signal levels. The stars denote the Raman lines related to the SRO buffer layer. Structural modes in bulk STO are marked with R. The arrows show positions of the zone center $TO_{2,3,4}$ phonons.

active below T_a due to the folding of the R point into the zone center at the phase transition [12,13]. Weak TO_2 and TO_4 peaks can also be seen in the single-crystal spectrum, likely due to the impurities in the sample.

The appearance of the strong TO phonon peaks indicates a lowering of the crystal symmetry in the STO films, the breaking of inversion, and/or translation symmetries. In STO single crystals, the inversion symmetry can be broken by applying an electric field [12] or by inducing ferroelectricity with the help of an external stress [13], impurities and defects [8,14], Ca doping [15], and, in another quantum paraelectric, $KTaO_3$ (KTO), Nb, and Li doping [16,17]. In the later cases, it has been attributed to the ferroelectric micro-ordered regions [15,17].

In our STO films, the lowering of the crystal symmetry is in part due to the lattice mismatch between the STO film and the SRO layer. One evidence of the strain effect caused by the lattice mismatch is the appearance of the silent nonpolar TO_3 phonon, which becomes Raman active only in the presence of a long-range lattice distortion of the order of phonon wavelengths [16]. The x-ray diffraction result, that the films are in the tetragonal structure, supports the existence of strain since without stress the structure of the single crystal should be cubic at room temperature [7]. The tetragonal phase is observed in films with thicknesses from 0.2–2.5 μm, suggesting that the effect of the lattice mismatch-induced strain extends to a large thickness. The persistence of the lattice mismatch-induced strain could be explained by the small mismatch between the STO film and the SRO layer (0.64%). This is also consistent with our dielectric measurements which show that the dielectric relaxation behaviors of STO thin films change continuously to large film thickness [3,18]. The R modes in the thin films are not detected, although it should exist in the tetragonal phase. It could be due to their weaker intensity compared to the Γ-point phonons. The symmetry of the thin films could also be even lower than the tetragonal structure due to strain. The possible orthorhombicity in the STO films should be very small, beyond the resolutions of both our polarization measurement and the x-ray diffraction. [We found no linear polarization in x-y and x'-y' coordinates at a circularly polarized excitation, and, at a linear polarized excitation, the $TO_{2,4}$ phonons were polarized along the excitation completely in the $z(x', x')\bar{z}$ and 80% in the $z(x, x)\bar{z}$ configurations.]

A uniform uniaxial strain does not break the inversion symmetry unless it exceeds the critical value ($\sim$1.6 kbar) for inducing ferroelectricity [13]. In our STO films, the lattice mismatch-induced strain is influenced by partial relaxation and defects and therefore this strain is most likely not uniformly distributed throughout the film, thus breaking the translation symmetry. The dielectric measurements of the STO films do not show a uniform ferroelectric phase. Instead, a diffused peak is observed in the ϵ'-T curves [4], suggesting nonuniform dielectric properties in the films. This is further conformed by x-ray diffraction that the superlattice peak associated with the tetragonal phase is very broad ($\sim$0.1°) [7]. An analysis of the optical phonon line shape indicates that the local lattice distortions in the STO films contribute to the lowering of the crystal symmetry. In Fig. 2, the enlarged spectra of the polar $TO_{2,4}$ and nonpolar TO_3 peaks for the 2.3 μm film are displayed for $T = 5$ K. The TO_2 peak is strongly asymmetric and exhibits a Fano profile: The scattering intensity increases at the high-energy side and is depressed at the low-energy side of the Raman peak. The dashed line is a fit using the following equation [19]:

$$I(\omega) = A\frac{[q + E(\omega)]^2}{1 + E(\omega)^2}, \qquad (1)$$

where $E(\omega) = 2(\omega - \omega_0)/\Gamma$. Here, ω_0 is the phonon frequency in the absence of interaction, Γ is its FWHM, A is the amplitude, and q is the asymmetry parameter, which is found to be positive in our spectra. In contrast, the TO_3 and TO_4 peaks shown in Figs. 2(b) and 2(c) are mostly symmetric, which corresponds to $q \to \infty$ and a Lorentzian shape with the intensity of the phonon line equal to Aq^2. Note that A and q are not independent and Aq^2 does not diverge with $q \to \infty$ (see Refs. [20,21] for details). The Fano effect occurs whenever discrete excitations and a broad continuum interfere coherently [19]. This continuum of excitations in STO films is polar because it interacts with the polar TO_2 phonon, but the nonpolar TO_3 phonon line is symmetric. Although TO_4 is polar, its energy is much higher, and most likely the

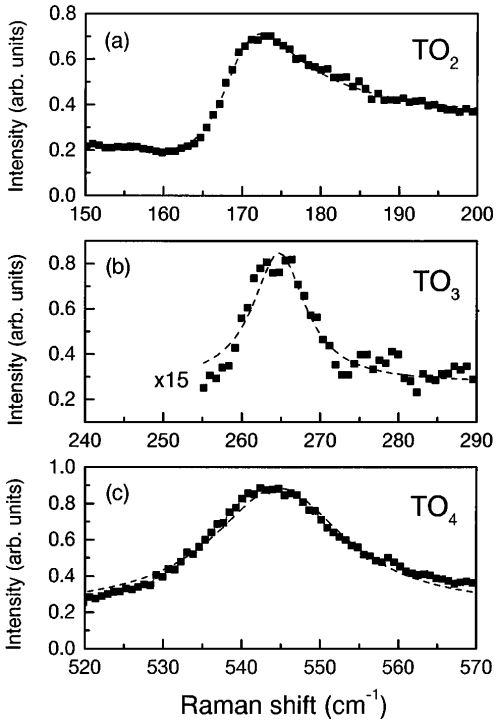

FIG. 2. (a) The Fano-like TO_2 peak for the 2.3 μm STO film at $T = 5$ K. Dashed lines represent fits to the Fano profile. (b),(c): The symmetric peaks for the TO_3 and TO_4 phonons, respectively. The linear background is subtracted for clarity.

density of states for the continuous excitation vanishes at the TO_4 frequency.

The possible continuous excitations that can interfere coherently with the optical phonons and give rise to the Fano asymmetry include electrons, as in semiconductors [20] and high-T_c superconductors [21], the two-acoustic-phonon states [22], or another TO phonon via acoustic phonons [23]. But these are unlikely the case for the STO films: The asymmetric factor q for the above effects are often negative, while it is positive in our results. In doped STO and KTO single crystals, the asymmetric line shape similar to that in Fig. 2(a) has also been found [16]. The polarization fluctuations in the defect-induced micropolar regions has been proposed to explain the asymmetry [15,17]. We believe that the Fano effect in our STO films results from the interaction of the TO_2 phonons with the polarization fluctuations in the micropolar regions. Since the optical phonons do not interact with *static* polarization, we postulate the existence of a wide spectrum of *rapid* polarization fluctuations with frequencies up to the TO_2-phonon frequency. This is different from the situation in Ref. [17], where the asymmetry is explained in terms of the *slow* modulations of the Raman tensor. The physical origin of the rapid polarization fluctuations is not currently clear, and the possibility that the soft optical modes are involved cannot be excluded.

Concerning the origin of the micropolar region, it is impossible to rule out the existence of impurities: Even in samples of highest purity, acceptor-type impurities have been detected [24]. The defect chemistry studies show, however, that the existence of these impurities, as well as cation off-stoichiometry, often results in oxygen vacancies in the titanates [24]. It was shown by Uwe *et al.* that when a nominally pure STO single crystal is reduced, ferroelectric microregions are induced in it [14]. In thin films, besides cation off-stoichiometry and acceptor-type impurities, oxygen vacancies can also result from insufficient oxygenation during the deposition process. Based on these considerations, we conclude that the micropolar regions in the STO films are most likely caused by the oxygen vacancies. It is difficult to precisely determine the oxygen content in a thin film. Using luminescence and optical second-harmonic generation measurements, Fischer *et al.* determined that the density of the dipolar microregions surrounding the oxygen vacancies is about 10^{17} cm^{-3} in well oxidized $KTaO_3$ single crystals [25]. The STO thin films in this work are highly resistive (resistivity is higher than 10^{13} Ω cm), which indicates a low free- carrier density. We can thus give a rough estimate of the oxygen vacancy density in the STO films to be of the order of 10^{17} cm^{-3}.

The soft TO_1 mode is expected to appear concurrently with other TO phonons. However, we did not detect any features that could be attributed to its presence. Instead, a broad maximum around 90 cm^{-1} was found between 5 and 100 K. Similar features have been reported in the reduced STO single crystals, and attributed to the defect-induced ferroelectric microregions [14].

In Fig. 3(a), q for the TO_2 peak is plotted as a function of temperature. It is nonzero at room temperature and increases as the temperature decreases. In theory [20,21], $q \sim 1/\rho_0$, where ρ_0 is the density of states for the continuous excitations at ω_0. Our result shows that ρ_0 does not vanish in the entire temperature region measured; hence, the rapid polarization fluctuations exist in the STO films even at room temperature. This could explain the existence of the dielectric nonlinearity in STO films up to room temperature, whereas in single crystals the nonlinearity (related to the hardening of the soft modes) vanishes above 70 K. We notice that the q-T curve is strikingly similar to the real part of the dielectric constant ϵ' versus T curve measured at 20 kHz in STO films, which is plotted in Fig. 3(b). In Fig. 3(c), we plot the temperature dependence of the $TO_{2,4}$ intensities [Aq^2 in Eq. (1)] divided by the corresponding statistical factor $n(\omega_0) + 1$ for the 2.3 μm film and the single crystal. A striking similarity is found between the thin film curves and the imaginary part of the dielectric constant ϵ'' versus T curve in STO shown in Fig. 3(b), in particular the distinct features at about 40 and 85 K. In comparison, the $TO_{2,4}$ peaks disappear around 30 K in the single crystal.

In conclusion, we have observed in STO thin films strong zone-center optical phonon peaks, symmetry

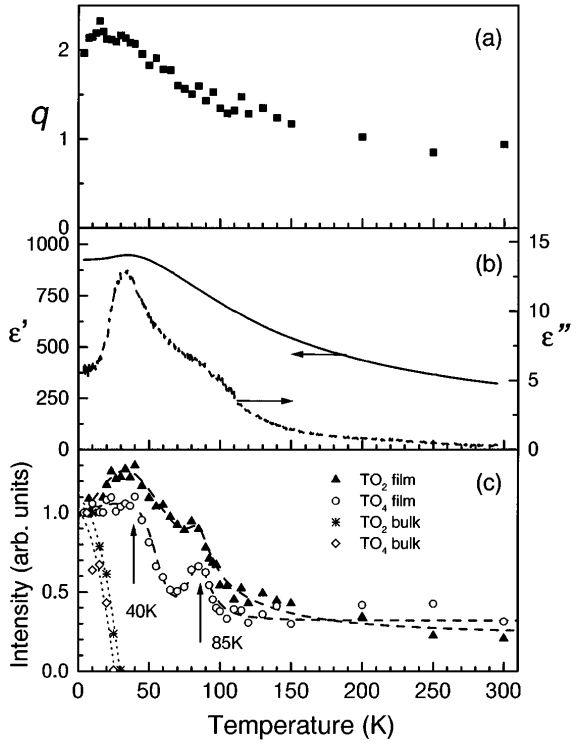

FIG. 3. (a) The temperature dependence of q for the 2.3 μm STO film. The result is strikingly similar to the ϵ'-T curve (b), suggesting that the density of continuous polar excitations in the micropolar regions does not vanish with temperature increase. (c) The temperature dependence of the TO_2 and TO_4 phonon intensities normalized by the corresponding statistical factor for the 2.3 μm STO film and the single crystal. The dashed lines guide the eye. Note the similarity to the ϵ''-T curve shown in (b).

forbidden in bulk STO. The TO_2 phonon shows a Fano asymmetry, which provides a convincing evidence to the existence of micropolar regions in the STO films. These regions exist up to room temperature, although they may change from dynamic to static (ferroelectric) at different temperatures. The lattice mismatch-induced strain and the oxygen vacancy-induced micropolar regions in the STO thin films have significant influence on their properties. The result is important for the understanding of the fundamental issues such as quantum fluctuations, structural phase transitions, and dielectric nonlinearity and loss of STO thin films.

The authors are grateful to V. Belitsky, H. Vogt, L. E. Cross, A. Bhalla, J. Levy, S. Shapiro, and B. Wells for helpful discussions. This work was partially supported by DOE under Grant No. DFFG02-84ER45095 and NSF under Grants No. DMR-9623315 and No. DMR-9702632.

*Permanent address: A. F. Ioffe Physico-Technical Institute, Russian Academy of Sciences, St. Petersburg 194021, Russia.

†Permanent address: National Laboratory for Superconductivity, Institute of Physics, Chinese Academy of Science, Beijing, People's Republic of China.

[1] K. A. Müller, W. Berlinger, and E. Tosatti, Z. Phys. B **84**, 277 (1991).
[2] E. Tosatti and R. Martoňák, Solid State Commun. **92**, 167 (1994).
[3] X. X. Xi *et al.* (to be published).
[4] H.-C. Li *et al.*, Appl. Phys. Lett. **73**, 190 (1998).
[5] A. K. Tagantsev, in *Ferroelectric Ceramics*, edited by N. Setter and E. L. Colla (Birkhäuser, Basel, 1993), p. 127.
[6] V. I. Merkulov *et al.*, Appl. Phys. Lett. **72**, 3291 (1998).
[7] B. O. Wells *et al.* (unpublished).
[8] W. G. Nilsen and J. G. Skinner, J. Chem. Phys. **48**, 2240 (1968).
[9] V. N. Denisov, B. N. Mavrin, and V. B. Podobedov, Phys. Rep. **151**, 1 (1987).
[10] H. Vogt and G. Rossbroich, Phys. Rev. B **24**, 3086 (1981); H. Vogt, *ibid.* **38**, 5699 (1988).
[11] D. Kirillov *et al.*, Phys. Rev. B **51**, 12 825 (1995).
[12] J. M. Worlock and P. A. Fleury, Phys. Rev. Lett. **19**, 1176 (1967).
[13] H. Uwe and T. Sakodo, Phys. Rev. B **13**, 271 (1976).
[14] H. Uwe *et al.*, Ferroelectrics **96**, 123 (1989).
[15] U. Bianchi *et al.*, J. Phys. Condens. Matter **6**, 1229 (1994).
[16] S. K. Manlief and H. Y. Fan, Phys. Rev. B **5**, 4046 (1972).
[17] J. Toulouse *et al.*, Phys. Rev. Lett. **68**, 232 (1992); P. DiAntonio *et al.*, Phys. Rev. B **47**, 5629 (1993).
[18] H.-C. Li *et al.*, Appl. Phys. Lett. **73**, 464 (1998).
[19] U. Fano, Phys. Rev. **124**, 1866 (1961).
[20] M. V. Klein, in *Light Scattering in Solids VI*, edited by M. Cardona (Springer-Verlag, Berlin, 1984), Vol. 54, p. 147.
[21] C. Tomsen, in *Light Scattering in Solids VII*, edited by M. Cardona and G. Güntherodt (Springer-Verlag, Berlin, 1991), Vol. 68, p. 285.
[22] D. L. Rousseau and S. P. S. Porto, Phys. Rev. Lett. **20**, 1354 (1968).
[23] A. Pinczuk *et al.*, Solid State Commun. **7**, 139 (1969).
[24] R. Waser and D. M. Smyth, in *Ferroelectric Thin Films: Synthesis and Basic Properties*, edited by C. P. de Araujo, J. F. Scott, and G. W. Taylor (Gordon and Breach, Amsterdam, 1996), p. 47.
[25] C. Fischer *et al.*, Radiat. Eff. Defects Solids **136**, 85 (1995).